



# Optimization of wear parameters on Ni–Al<sub>2</sub>O<sub>3</sub> nanocomposite coating by electrodeposition process

C. R. Raghavendra<sup>1</sup>  · S. Basavarajappa<sup>2</sup> · Irappa Sogalad<sup>3</sup>

© Springer Nature Switzerland AG 2018

## Abstract

The present work concentrates on the nanocomposite coating on the mild steel substrate. The mild steel substrate demands good surface preparation in order to have better adhesive strength of coating. In the light of this, surface is grinded and cleaned later followed by rinsing. In this work, Ni–Al<sub>2</sub>O<sub>3</sub> composite coating was successfully coated on mild steel (AISI 1018) substrate. The study on different wear parameters on the specific wear rate is carried on. The experimental design is carried out with 20 trails as per central composite design considering normal load, sliding speed and sliding distance on the samples. The morphology of surface after coating and wear analysis is studied. The results revealed higher wear resistance by the presence of nano-Al<sub>2</sub>O<sub>3</sub> particles in the Ni matrix composite coating. The effect of normal load and its interaction with sliding distance are found to be more effective on specific wear rate. The abrasive nature of wear is observed due to the presence of hard Al<sub>2</sub>O<sub>3</sub> nanoparticles embedded in the Ni matrix. The chemical composition and distribution of particle analysis is carried out by SEM and EDS micrograph.

**Keywords** Ni–nano-Al<sub>2</sub>O<sub>3</sub> coating · Specific wear rate · Response surface method

## 1 Introduction

The main aim of the coating is to improve the surface properties of the substrate material. In any engineering component, the surface is one of the very important parts. The most of the machine components fails due to surface defects such as wear, corrosion and fatigue. The property of coating depends on the type of (micro/nano) particles embedded in the matrix. The significance of coating with reinforcement particles is to increase/enhance properties, viz. tribological, mechanical and corrosion resistance [1–3]. The substrate and the coating materials are connected to cathode and anode terminals respectively during the electrodeposition process. Insight the materials used as the coating and substrate materials needs to be electrically conductive in nature [4]. This coating provides a wide range of choices using the variety of materials for different

applications in automobile and industrial applications due to better tribological and corrosion properties [5]. With the addition of incorporated particles in the coating, the main coating metal plays a vital role in adhesive strength with base material [6]. The presence of micro/nanohard particles in metal matrix is highlighted due to their excellent tribological property [7–9]. The Ni–Al<sub>2</sub>O<sub>3</sub> coatings are repeatedly proved to be an effective coating in enhancing the life of substrate material in the abrasive environment which are carried out by electro-co-deposition process [10–14]. It is evident from the literature that many researchers have concentrated on nano-Al<sub>2</sub>O<sub>3</sub> coating matrix in different fields of applications on different materials. Though the presence of hard particles in the coating is proved to be better surface protection against wear, the study on intensity and role of wear parameters on composite coating is limited. In the present work, an

✉ C. R. Raghavendra, raghavendra.crclk@gmail.com | <sup>1</sup>Department of Mechanical Engineering, Government Engineering College, Haveri, Karnataka, India. <sup>2</sup>Indian Institute of Information Technology, Dharwad, IT Park, Hubballi, Karnataka, India. <sup>3</sup>University BDT College of Engineering, Davanagere, Karnataka, India.

approach towards coating of Ni–nano- $\text{Al}_2\text{O}_3$  composite on AISI 1018 mild steel substrate which is widely used for fixtures, mounting plates and spacers is concentrated. The specific wear rate behaviour of corresponding composite coating is analysed. Further, influence of wear parameters, viz. normal load, sliding speed and sliding distance on the composite coating, is carried on.

## 2 Experimental procedure

### 2.1 Substrate preparation

The quality of the surface finish plays a foremost role in adhesive strength of coating on the substrate. The substrate is taken as per American Society for Testing and Materials (ASTM) G99 standard for wear having 10 mm diameter and 30 mm length. In the light of achieving better adhesion of Ni– $\text{Al}_2\text{O}_3$  composite coating, the substrate is well polished and rough grinded. For this purpose, different grit sizes of SiC emery papers are used for polishing with a speed of rotation 400 rpm. Then, the substrate is cleaned in demineralized (DM) water, degreased and eroded in sodium hydroxide (NaOH) at atmospheric temperature.

The electrolyte bath for Ni coating is prepared as per Watts bath standard with the following composition: nickel sulphate ( $\text{NiSO}_4$ ) 250 g/L; nickel chloride ( $\text{NiCl}_2$ ) 45 g/L; and boric acid ( $\text{H}_3\text{BO}_3$ ) 30 g/L [15–23]. The bath is prepared for 1 lit each for every sample in order to maintain the quality and homogeneity of the coating. The pure nickel (purity 99.98%) dimensions of  $12 \times 8 \text{ mm}^2$  plate with 5 mm thickness is considered as anode, and substrate with Ni– $\text{Al}_2\text{O}_3$  composite coating AISI 1018 is used as cathode. The distance between the anode and cathode

is maintained by 9 cm. Further  $\text{Al}_2\text{O}_3$  nanoparticles (Reinste, Pvt. Ltd., India) of size 40 nm are used. The operating conditions of electro-co-deposition are given in Table 1. The  $\text{Al}_2\text{O}_3$  nanoparticle distributions and morphology are carried out using scanning electron microscopy (SEM).

The response surface methodology (RSM) is a collection of statistical and mathematical techniques useful for developing, improving and optimizing processes. CCD method is very effective in designing the experiments effectively. The experimental design of the wear parameters, viz. normal load applied, sliding speed and sliding distance, is considered as the three variables in the five levels each which are shown in Table 2. The normal load on the pin is applied by the linear variable differential transformer (LVDT) at the end of the hanger to which the pin is fixed. According to CCD 20, number of trials are experimented for which the electro-co-deposition is carried out at fixed operating conditions; the corresponding values are given in Table 1.

## 3 Results and discussion

### 3.1 Morphology study

Figure 1a, b shows the micrograph images taken in scanning electron microscopy (SEM) of coating surfaces at different magnifications. It is evident that the presence and distribution of Ni and  $\text{Al}_2\text{O}_3$  is found to be uniform and homogeneous. The images at different magnifications are considered for the morphology study in order to confirm the uniform coating obtained for the specimen. It is also observed that there was no sign of agglomerated particle on the surface of coating. This encourages the better accuracy of specific wear rate values. Further energy-dispersive spectroscopy (EDS) is used to study the quantitative analysis of composite coating. Figure 1c shows the EDS image which confirms the presence and distribution of Ni and  $\text{Al}_2\text{O}_3$  particles on the coating surface. The quantitative analysis of Ni– $\alpha$ - $\text{Al}_2\text{O}_3$  composite coating is shown in Fig. 3d and found to be 91.54% of Ni, 2.34% of Al and 6.12% of O in weight basis. In order to study the particle distribution over the volume of the coating, the cross-sectional image of the coating is considered. Figure 2 shows

**Table 1** Operating conditions

Sl. no.	Operating parameters	Quantity
1	Bath temperature ( $^{\circ}\text{C}$ )	40
2	Current density ( $\text{A}/\text{dm}^2$ )	1.5
3	Particle concentration ( $\text{Al}_2\text{O}_3$ ) (g/L)	4.5
4	pH	3–4
5	Stirring speed (rpm)	250

**Table 2** Coded and uncoded values of experiment

Factors	Symbols coded	Encoded values of coded levels				
		–1.682	–1	0	1	1.682
Normal load (N)	$X_1$	10	18	30	41	50
Sliding speed (rpm)	$X_2$	200	321	500	678	800
Sliding distance (m)	$X_3$	1000	1405	2000	2594	3000

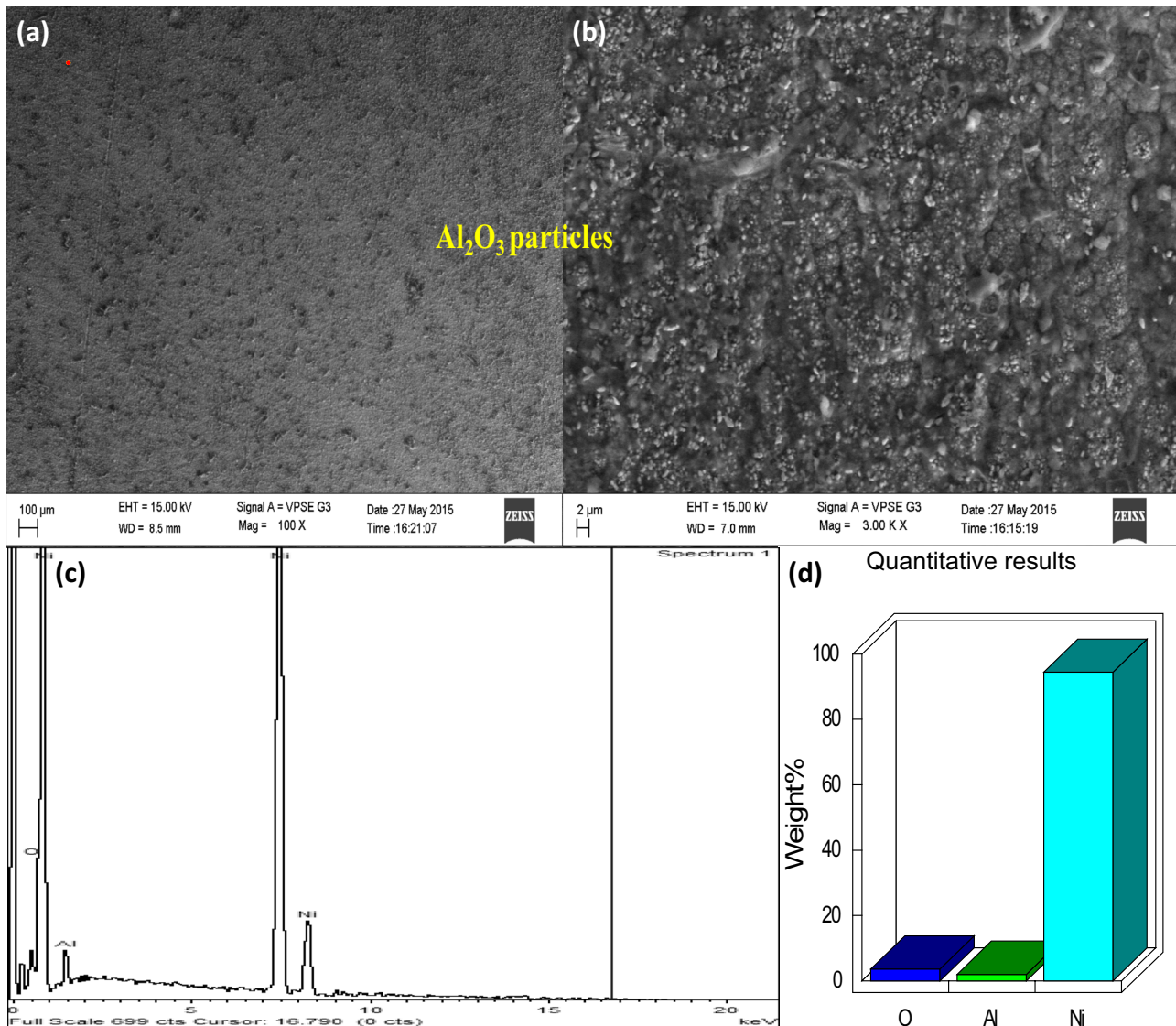


**Fig. 1** Scanning electron micrograph of the surface of a Ni-Al<sub>2</sub>O<sub>3</sub> composite coating by electrodeposition **a** × 100, **b** × 3000, **c** EDS analysis, **d** chemical composition of the coating on wt%

particle distribution along the depth of the coating and also witnesses the uniform thickness of the coating.

### 3.2 Wear test

The dry sliding wear tests are conducted on pin-on-disc test rig (Ducom, Pvt. Ltd., India). Initially, the test sample is weighed in weighing machine having 0.001 g least count before and after wear. The difference in the weight is used to calculate specific wear rate in terms of mm<sup>3</sup>/N m. The wear tests are conducted for the samples without coating (bare sample) and without nano-Al<sub>2</sub>O<sub>3</sub> particles, i.e. sample with Ni coating. The specific wear of the corresponding samples is found to be 0.018 mm<sup>3</sup>/N m and 0.0101 mm<sup>3</sup>/N m, respectively. The

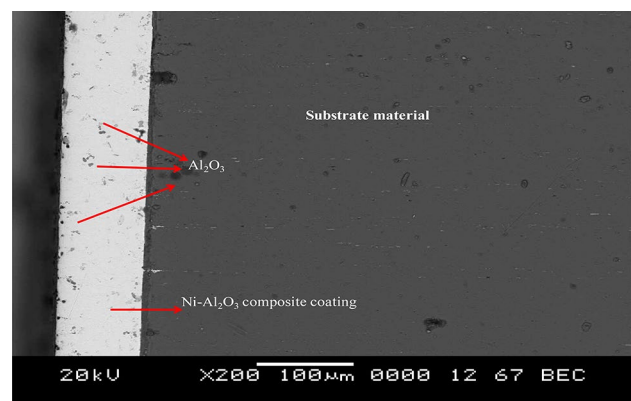


**Fig. 2** SEM micrograph image of Ni-Al<sub>2</sub>O<sub>3</sub> composite coating cross section

operating conditions of 20 N, 200 rpm and 1000 m of normal load, sliding speed and sliding distance, respectively, are maintained during tests. Later the wear tests are conducted as per the CCD of the design plan as shown in Table 3. It is found that there is an increase of 43.88% in the specific wear rate with Ni coating in comparison with bare sample.

**Table 3** Design plan for wear test as per CCD

Sl. no.	Load (N)	Hertzian pressure (MPa)	Speed (rpm)	Sliding distance (m)
1	18	1167.8	321	2594
2	10	960	500	2000
3	18	1167.8	321	1405
4	30	1209.6	500	2000
5	30	1209.6	500	1000
6	30	1209.6	500	2000
7	41	1536.5	678	2594
8	30	1209.6	500	2000
9	30	1209.6	200	2000
10	50	1641.6	500	2000
11	18	1167.8	678	2594
12	18	1167.8	678	1405
13	41	1536.5	678	1405
14	41	1536.5	321	1405
15	30	1209.6	500	2000
16	41	1536.5	321	2594
17	30	1209.6	500	3000
18	30	1209.6	500	2000
19	30	1209.6	500	2000
20	30	1209.6	800	2000

### 3.3 Influence of operating parameters on the specific wear rate

The experiments are designed for 95% confidence level; it means that the obtained models are considered to be statistically significant. The term R-squared or coefficient of determination ( $R^2$ ) measures the degree of fitness of the experimental variations. The higher the value of  $R^2$  indicates the better fits with the actual data [24]. From Fig. 3a, it is evident that the normal load applied is more influencing on the specific wear rate followed by the sliding distance. The normal load applied is contributing 18.68% followed by sliding distance and speed contributing 17.29 and 10.17%, respectively. The sliding speed has the least influence on the wear rate. The interaction effect (shown in Fig. 3b) of load with speed is more predominant on specific wear rate followed with interaction with the sliding distance, whereas the interaction effect of sliding speed and sliding distance is least. The highest contribution of 25.03% is found for the interaction effect of load with the speed followed by 19.03% for the interaction effect of load with sliding distance.

In general, the  $R^2$  measures the percentage of variation of data which is explained by the regression equation and it is useful while comparing models with different numbers of terms. For the specific wear rate the determination coefficient  $R^2$  is found to be 94.99% of the variability in the response. This symbolizes higher statistical significance associated with prediction and achieved values by experiment. Also, the adjusted  $R^2$  (90.49%) is also close to expected value of  $R^2$ .

The difference in the actual and expected values is shown by normal probability plot. Figure 4a shows the normal probability plot where the point of experimental values lies within the range. The residual fitness in the model is shown in Fig. 4b. The specific wear rate is considered as

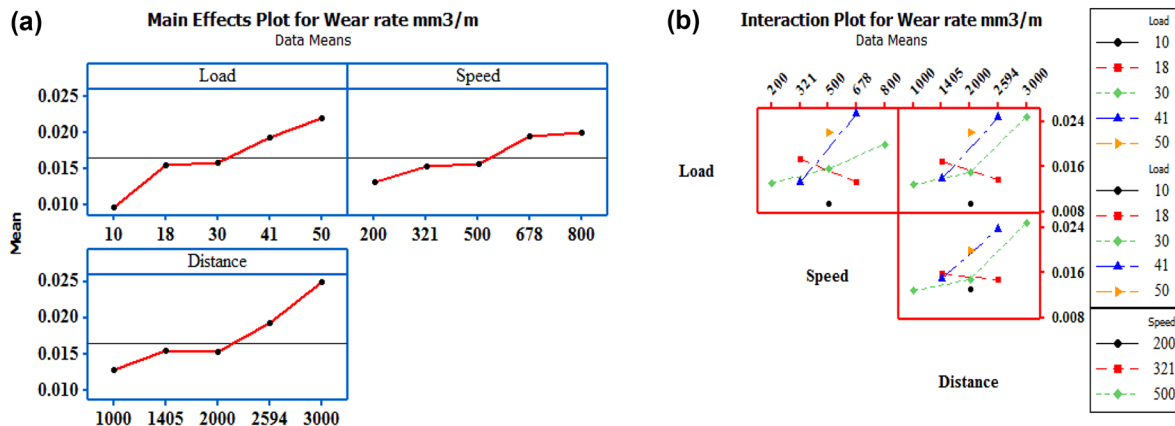
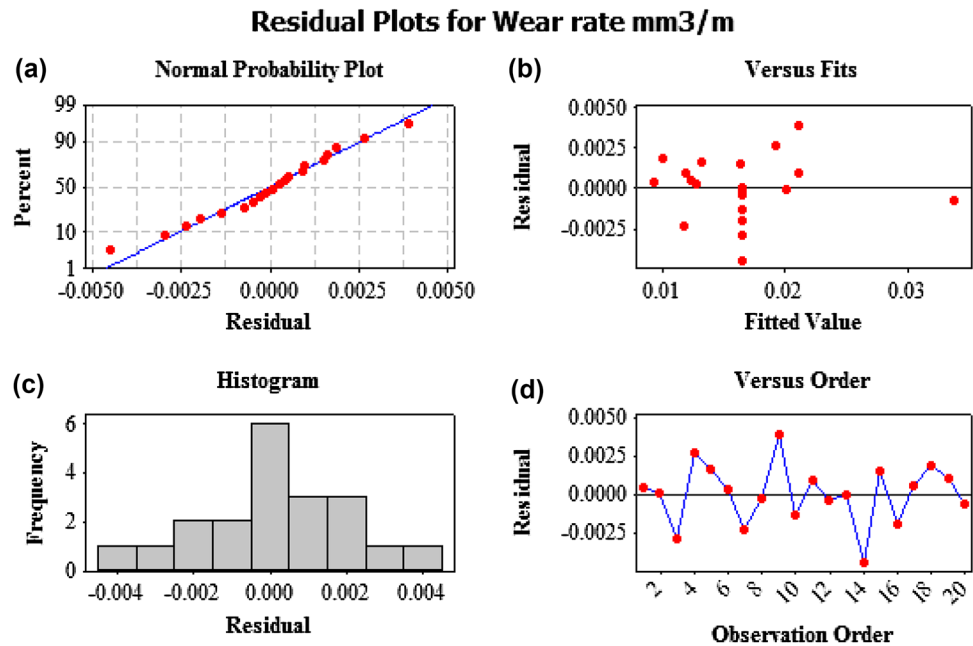


**Fig. 3** a Main effect plot for wear rate and b interaction plot for wear rate

**Fig. 4** **a** Normal probability plot, **b** residual versus fits, **c** histogram, **d** residual versus order of wear rate against wear parameters



the dependent variable, whereas the pin surface and wear parameters are considered as the independent. Figure 4c shows the histogram of the frequency against the residual errors. Symmetrical bell shape is observed which indicates good fit in the regression. This is also supported by Fig. 4d where the residual error falls within and around the mean range for all the 20 trails.

### 3.4 Wear mechanism

Figure 5 shows the 3-D surface plots of interaction effect of normal load, sliding speed and sliding distance on

the wear rate of Ni–Al<sub>2</sub>O<sub>3</sub> composite coating. It has been observed that the wear rate is minimum at lower load and increases with the increase in the load applied and similar trend is followed by the speed and the distance of sliding. The minimum wear rate observed is 0.000244 mm<sup>3</sup>/N m at 41 N, 321 rpm and 1405 m and the maximum is 0.0012 mm<sup>3</sup>/N m at 18 N, 321 rpm and 1405 m. The operating parameters in wear such as the Hertzian pressure given in Table 3 were chosen mild and close to the practical dry sliding conditions in the light of observing the nature of debris in the contact zone.

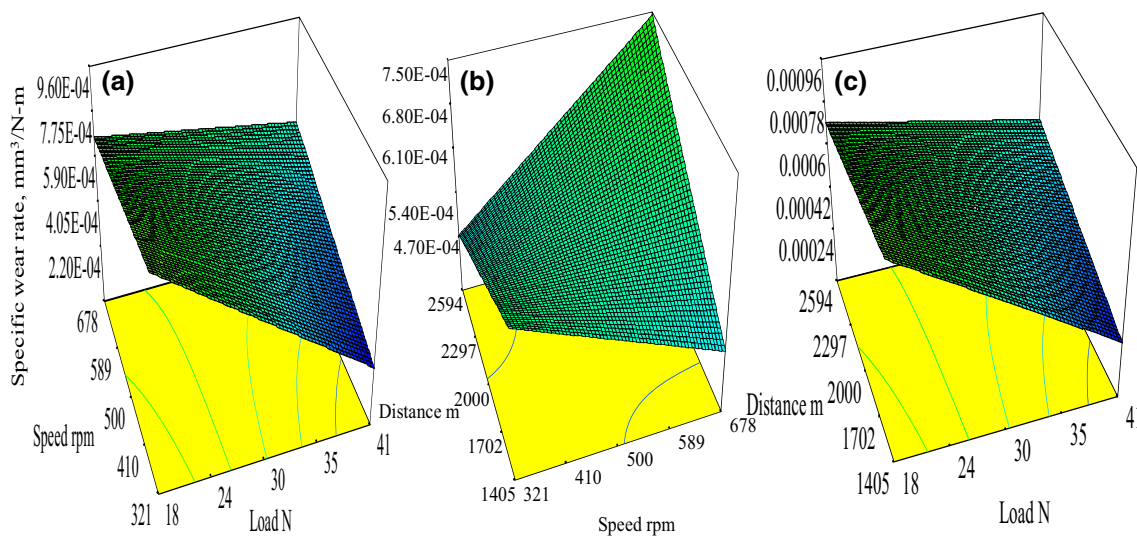


**Fig. 5** 3-D surface plots showing the influence of load, speed and sliding distance on the wear rate

The applied load in the dry sliding wear is more predominant [25]. The  $Al_2O_3$  particles in deposit are influencing on the wear resistance [26], and the abrasive nature of wear is highlighted due to the presence of hard particles. The increase in the load increases the load on the asperities which are actually in contact with the counter body (disc). This may lead to smear out asperities leading to more surface contact and higher wear rate. This is evident from Fig. 6a that, at lower load and sliding distance, the scratch marks are along the direction of rotation with less ploughing effect. It is natural to observe higher wear rate at higher sliding distance due to more debris getting entrapped between the pin and counter-surface (Fig. 6b and c) showing significant removal of material with higher depth and width of grooves which symbolizes the degree of size and quantity of debris accumulated in the worn out surface. This is may be due to the higher resistance offered by the nano- $Al_2O_3$  particles in the Ni matrix, as these nanoparticles are harder than the Ni particles, which can pluck out of coating at higher load and sliding distance. Furthermore, increasing the load of the wear test for the composite coating, as shown in Fig. 6c, continuous abrasive grooves are significantly increased. The wear tracks shows surface with scratch marks under the applied load of 10 N. These are found rough in nature as compared to the wear track surface under the applied load of 50 N. This is due to the debris fragments formed at 50 N load which are conglomerated wear particles. This can be the results of plastic shearing and detachment mechanism which may occur during the course of sliding. Figure 6b shows the SEM image where the debris produced under

an applied load of 30 N is highlighted. The further compression of the pin has resulted in the flat and elongated debris leading to shearing due to the dry sliding. This is attributed by the presence of nano- $Al_2O_3$  particles in the composite coating. Figure 7 shows the drastic change in the specific wear rate in comparison with the sample without coating and without nanoparticles in the Ni coating. Even the maximum specific wear of Ni- $Al_2O_3$  coating is much less than the Ni-coated samples. The presence of Ni- $Al_2O_3$  composite coating even after the sliding wear is witnessed by the EDS image shown in Fig. 8. This provides the evidence of resistance of the composite coating provided against the dry sliding wear. The wt% quantitative analysis revealed the presence of Ni by 87.43%, Al by 4.11% and O by 8.46%.

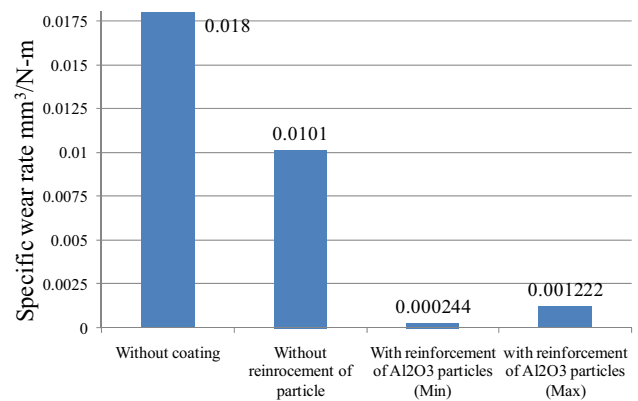


Fig. 7 Comparison results of specific wear rate

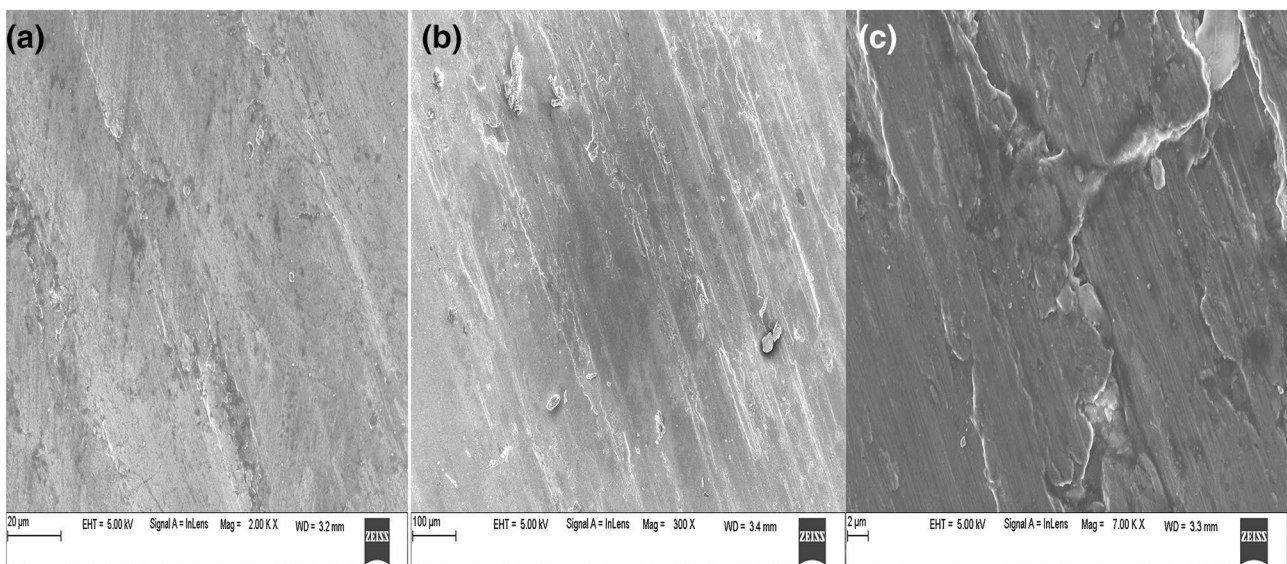
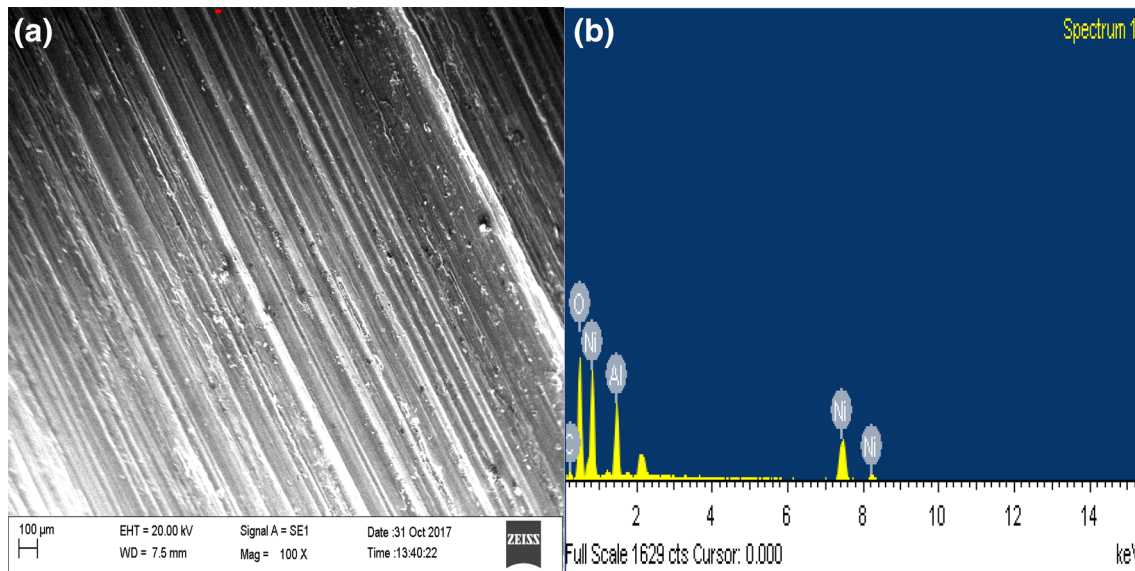


Fig. 6 a 10 N, b 30 N and c 50 N wear tracks at different loads



**Fig. 8** **a** Worn out surface and **b** EDS image of worn out surface

## 4 Conclusions

In summary, Ni–Al<sub>2</sub>O<sub>3</sub> composite coating is prepared with good adhesive strength by electro-co-deposition method. The presence of Al<sub>2</sub>O<sub>3</sub> nanoparticles has increased wear resistance compared to Ni coating. The different wear parameters have significant influence on the specific wear rate at different levels. The outcomes of the work are listed below: (1) normal load applied on the pin has foremost influence on the specific wear rate which is followed by its interaction effect with sliding distance and sliding speed; (2) specific wear rate is less at lower load, speed and distance at 10 N, 200 rpm and 1000 m; and (3) at more load, severe wear is observed with wider and deeper wear tracks.

## Compliance with ethical standards

**Conflict of interest** The authors declare that there are no conflicts of interest.

## References

- Raghavendra CR, Basavarajappa S, Sogalad I (2016) Electrodeposition of Ni–Al<sub>2</sub>O<sub>3</sub> nano composite coating and evaluation of wear characteristics. IOP Sci. <https://doi.org/10.1088/1757-899x/149/1/012110>
- Yao Y, Yao S, Zhang L, Wang H (2007) Electrodeposition and mechanical and corrosion resistance properties of Ni–W/SiC nanocomposite coatings. Mater Lett 61:67–70
- Zhen J, Li F, Zhu S, Ma J, Qiao Z (2014) Tribology International Friction and wear behavior of nickel-alloy-based high temperature self-lubricating composites against Si 3 N 4 and Inconel 718. Tribol Int 75:1–9
- Mellor BG (2006) Surface coatings for protection against wear. Woodhead Publishing Limited, Cambridge
- Thiemig D, Bund A, Talbot JB (2009) Influence of hydrodynamics and pulse plating parameters on the electrocodeposition of nickel–alumina nanocomposite films. Electrochim Acta 54:2491–2498
- Feng Q, Li T, Yue H, Qi K, Bai F, Jin J (2008) Preparation and characterization of nickel nano-Al<sub>2</sub>O<sub>3</sub> composite coatings by sediment co-deposition. Appl Surf Sci 254:2262–2268
- Srivastava M, Grips VKW, Jain A, Rajam KS (2007) Influence of SiC particle size on the structure and tribological properties of Ni–Co composites. Appl Surf Sci 202:310–318
- Narasimman P, Pushpavanam M, Periasamy VM (2011) Synthesis, characterization and comparison of sediment electrocodeposited nickel–micro and nano SiC composites. Appl Surf Sci 258:590–598
- Rostami M, Fahami A, Nasiri-tabrizi B, Ebrahimi-kahrizsangi R (2013) Characterization of electrodeposited Ni–SiC–C g nanocomposite coating. Appl Surf Sci 265:369–374
- Chen L, Wang L, Zeng Z, Zhang J (2006) Effect of surfactant on the electrodeposition and wear resistance of Ni–Al<sub>2</sub>O<sub>3</sub> composite coatings. Mater Sci Eng, A 434:319–325
- Gül H, Kilic F, Aslan S, Alp A, Akbulut H (2009) Characteristics of electro-co-deposited Ni–Al<sub>2</sub>O<sub>3</sub> nano-particle reinforced metal matrix composite (MMC) coatings. Wear 267:976–990
- Starosta R, Zielinski A (2004) Effect of chemical composition on corrosion and wear behaviour of the composite Ni–Fe–Al<sub>2</sub>O<sub>3</sub> coatings. J Mater Process Technol 157–158:434–441
- Shrestha NK, Sakurada K, Masuko M, Saji T (2001) Composite coatings of nickel and ceramic particles prepared in two steps. Surf Coat Technol 140:175–181
- Sasi A, Mondal M, Dayal S, Kumar S (2015) Electro deposition of nickel–alumina composite coating. Mater Today Proc 2:3042–3048
- Yang YF, Gong ZQ, Deng LY, Luo BP, Ma YT, Yang ZH (2006) Electrodeposition of Ni–Cr alloy on aluminum substrate. J Cent South Univ Technol (English Ed) 13(3):219–224

16. Lajevardi SA, Shahrabi T (2010) Effects of pulse electrodeposition parameters on the properties of Ni-TiO<sub>2</sub> nanocomposite coatings. *Appl Surf Sci* 256(22):6775–6781
17. Lv B, Hu Z, Wang X, Xu B (2015) Electrodeposition of nanocrystalline nickel assisted by flexible friction from an additive-free Watts bath. *Surf Coat Technol* 270:123–131
18. Gyftou P, Pavlatou EA, Spyrellis N (2008) Effect of pulse electrodeposition parameters on the properties of Ni/nano-SiC composites. *Appl Surf Sci* 254:5910–5916
19. Garcia I, Conde A, Langelaan G, Fransaer J, Celis JP (2003) Improved corrosion resistance through microstructural modifications induced by codepositing SiC-particles with electrolytic nickel. *Corros Sci* 45:1173–1189
20. Socha RP, Nowak P, Laajalehto K, Väyrynen J (2004) Particle-electrode surface interaction during nickel electrodeposition from suspensions containing SiC and SiO<sub>2</sub> particles. *Colloids Surf A Physicochem Eng Asp* 235:45–55
21. El-sherik AM, Shirokoff J, Erb U (2005) Stress measurements in nanocrystalline Ni electrodeposits. *J Alloys Compd* 389:140–143
22. Spanou S, Pavlatou EA (2010) Pulse electrodeposition of Ni/nano-TiO<sub>2</sub> composites: effect of pulse frequency on deposits properties. *J Appl Electrochem* 40:1325–1336
23. Bahrololoom ME, Sani R (2005) The influence of pulse plating parameters on the hardness and wear resistance of nickel – alumina composite coatings. *Surf Coat Technol* 192:154–163
24. Neşeli S, Yaldiz S, Türkeş E (2011) Optimization of tool geometry parameters for turning operations based on the response surface methodology. *Meas J Int Meas Confed* 44(3):580–587
25. Basavarajappa S, Ellangovan S, Arun KV (2009) Studies on dry sliding wear behaviour of graphite filled glass-epoxy composites. *Mater Des* 30(7):2670–2675
26. Raghavendra CR, Basavarajappa S, Sogalad I (2016) Electrodeposition of Ni-Al<sub>2</sub>O<sub>3</sub> nano composite coating and evaluation of wear characteristics. In: IOP conference series: materials science and engineering, vol 149, no 1